Applied Physics Letters ARTICLE scitation.org/journal/apl

Interface of Sn-doped $AgAlTe_2$ and $LiInTe_2$: A theoretical model of tandem intermediate band absorber

Cite as: Appl. Phys. Lett. **118**, 043901 (2021); doi: 10.1063/5.0034852
Submitted: 26 October 2020 · Accepted: 7 January 2021 ·
Published Online: 25 January 2021

View Online Export Citation CrossMark

Dan Huang,[1,a)] Lijie Ding,[1] Yang Xue,[1] Jin Guo,[1] Yu-Jun Zhao,[2,a)] and Clas Persson[3,4,a)]

AFFILIATIONS

[1]Guangxi Key Laboratory for Relativistic Astrophysics, Guangxi Colleges and Universities Key Laboratory of Novel Energy Materials and Related Technology, Guangxi Novel Battery Materials Research Center of Engineering Technology, Guangxi Key Laboratory of Processing for Non-Ferrous Metallic and Featured Materials, School of Physical Science and Technology, Guangxi University, Nanning 530004, People's Republic of China

[2]Department of Physics and Key Laboratory of Advanced Energy Storage Materials of Guangdong Province, South China University of Technology, Guangzhou 510640, People's Republic of China

[3]Department of Physics and Centre for Materials Science and Nanotechnology, University of Oslo, P.O. Box 1048 Blindern, NO-0316 Oslo, Norway

[4]Department of Materials Science and Engineering, Royal Institute of Technology, SE-100 44 Stockholm, Sweden

Note: This paper is part of the APL Special Collection on Scalable Ways to Break the Efficiency Limit of Single-Junction Solar Cells.
[a)]**Authors to whom correspondence should be addressed:** danhuang@gxu.edu.cn, zhaoyj@scut.edu.cn and clas.persson@fys.uio.no

ABSTRACT

Designing a new absorber to overcome the Shockley–Queisser limit for single-junction solar cells is of great importance for solar cell advancements. Here, a theoretical model of tandem intermediate band absorber is proposed based on the interface of Sn-doped $AgAlTe_2$ and $LiInTe_2$. Sn-doped $AgAlTe_2$ and $LiInTe_2$ are imminent to produce ideal heterojunctions as they possess similar lattice constants and the type-II band offset, providing an approach to overcome the Shockley–Queisser limit.

In the past few decades, solar energy has been paid much attention as being a renewable and clean energy resource and regarded as the ultimate way to solve the energy and environment crisis.[1] A solar cell as a device transferring sunlight to electricity directly has attracted great interest in research and industry communities.[2] The power conversion efficiency of the solar cell using chalcopyrite $Cu(In, Ga)Se_2$ as the absorber material has been achieved 22.6%.[3] More recently, the efficiency of the organic–inorganic hybrid perovskite solar cell has experienced a fast increase and reached beyond 23%.[4] However, the efficiency of the single junction solar cell is restricted to 31.0% at one sun concentration by the SQ (Shockley and Queisser) theoretical limit[5] owing to the broad spectral distribution of solar radiation, which limits the development space of thin-film solar cells.

To increase the efficiency of the solar cell, a few innovative proposals like tandem solar cells,[6] intermediate band (IB) solar cells,[7,8] hot carrier solar cells,[9] etc., have been raised. The tandem solar cell exceeds the SQ efficiency limit of the single-junction solar cell by using multiple absorber materials with different bandgap energies. Therefore, different absorber layers with various bandgap energies can absorb photons with different energies and then cover the solar light spectrum effectively. For example, a 47.1% conversion efficiency under 143 suns concentration has been realized in a six-junction III–V tandem solar cell.[10] However, this efficiency is achieved at the expense of increased growth complexity and manufacturing cost. In 1997, the concept of intermediate band solar cells (IBSCs) was proposed by Luque and Marti,[7] through introducing a partially filled IB into the main bandgap of the host semiconductor to enable a three-photon absorption process in one absorber material. Therefore, the electrons can be excited not only from the original valence band (VB) to the conduction band (CB) but also from the VB to the IB and from the IB to the CB. As a result, the photocurrent of the IBSC increases without sacrificing the photovoltage. The maximum theoretical efficiency of the IBSC with one IB increases remarkably over the SQ limit to 46.8% at one sun illumination and 63.2% at full concentration.[11] At present,

doping a suitable element with a high concentration in the host semiconductor is regarded as the feasible way to induce an IB in the original bandgap. Several doped semiconductors like Ti-,[12] Cr-,[13] Fe-,[14] and Sn-doped[15] $CuGaS_2$, Ti-[16] and V-doped[17] SnS_2, V-doped In_2S_3,[18] O-doped ZnTe,[19,20] etc., have been studied experimentally in which distinct sub-gap absorptions related to the IB have been observed. Interestingly, no study has been reported to couple these two approaches (i.e., tandem and intermediate band) to design a tandem intermediate band absorber, which is clearly expected to absorb more photons with less absorber layers.

To design a tandem intermediate band absorber, first, we need to find two different semiconductors, which can form a half-filled and delocalized IB after a heavy doping. Second, the IB position and then the sub-bandgaps of the intermediate band absorbers should be suitable to absorb the photons with different energies to cover the solar light spectrum effectively. Third, the two host semiconductors should possess similar crystal structures and lattice constants to avoid serious lattice mismatch. Fourth, a type-II band offset between the two adopted host semiconductors is required to facilitate light-generated electron and hole separation. In our earlier work,[21] we found that Sn is easily doped at the Al site in $AgAlTe_2$ and reaches a large doping concentration to form an IB. Due to the ideal IB position resulting from Sn doping, the values of the main bandgap and sub-bandgaps have a reasonable distribution and then the absorption coefficient of Sn-doped $AgAlTe_2$ can cover the solar light spectrum effectively. Moreover, with the Sn-doping concentration increasing in $AgAlTe_2$, the center of the intermediate band would not have a significant change while the width of the intermediate band and the absorption coefficient will have an increase. Therefore, Sn-doped $AgAlTe_2$ with a chalcopyrite structure has been suggested as a promising intermediate band absorber.[21] We notice that $LiXTe_2$ (X = Al, Ga, In) compounds have the same chalcopyrite structure and similar lattice constants to $AgAlTe_2$ and it is possible to design a tandem intermediate band absorber from the heterojunction by these compounds.

In this Letter, we have theoretically studied the electronic structure of $LiXTe_2$ (X = Al, Ga, In) and found interestingly that $LiInTe_2$ possesses a type-II band offset with $AgAlTe_2$ and an isolated and half-filled IB when doped with Si, Ge, or Sn at In sites. Further studies reveal that Sn-doped $LiInTe_2$ is a promising intermediate band absorber capable of high doping concentration. As the type-II band offset is preserved between Sn-doped $AgAlTe_2$ and $LiInTe_2$, the corresponding tandem intermediate band absorber is proposed for high efficiency solar cells. Of note, our proposed tandem model is based on connecting two intermediate band absorbers other than two solar cells. This is different from usual tandem solar cells, where a tunneling layer is required to connect the different solar cells (multiply p–n junctions).[10]

We notice that $LiXTe_2$ (X = Al, Ga, and In) and $AgAlTe_2$ have similar lattice constants (c.f. Table S1). In particular, the differences of *a* and *b* between $LiXTe_2$ (X = Al, Ga, and In) and $AgAlTe_2$ are all less than 2%. Heterojunctions between $LiXTe_2$ (X = Al, Ga, and In) and $AgAlTe_2$ along the [001] direction are expected to avoid serious lattice mismatch. In addition to the crystal structure, the electronic structure of $LiXTe_2$ (X = Al, Ga, and In) is another criterion to single out the component of the heterojunction to match $AgAlTe_2$. All the calculated band structures of $LiXTe_2$ (X = Al, Ga, and In) possess direct bandgaps (c.f. Fig. S1). The HSE06 calculated bandgaps are 3.112, 2.497, and 2.223 eV for $LiAlTe_2$, $LiGaTe_2$ and $LiInTe_2$, respectively, in line with the experimental results[22–25] and available theoretical results based on advanced methods,[25–28] as listed in Table S1. It is well known that the traditional calculation methods like local density approximation (LDA), generalized gradient approximation (GGA), and GGA+U (correction with an on-site Coulomb interactions) underestimate the bandgaps of semiconductors.[29] After adopting advanced methods like modified Becke–Johnson exchange potential (mBJ) and hybrid functional (HSE06 and B3PW91), one can obtain reasonable bandgaps compared with experiment. Therefore, the bandgaps from HSE06 calculations are adopted for further studies in this work. The bandgap of $LiAlTe_2$ is not suitable for the host of the IBSC, while the bandgaps of $LiGaTe_2$ and $LiInTe_2$ are close to the ideal values of bandgaps (2.40 eV at one sun concentration and 1.93 eV at full concentration)[30,31] for the IBSC.

In order to estimate the band edge positions of $LiXTe_2$ (X=Al, Ga, and In) with respect to the vacuum, we adopt the ionization potential of $AgAlTe_2$ (6.05 eV) from our earlier work[32] and then calculate the band offsets between $AgAlTe_2$, $LiAlTe_2$, $LiGaTe_2$, and $LiInTe_2$. Figure 1 presents band edge positions relative to vacuum of $AgAlTe_2$, $LiAlTe_2$, $LiGaTe_2$, and $LiInTe_2$. One observes that the valence band position of $AgAlTe_2$ is higher than those of $LiXTe_2$ (X=Al, Ga, and In). The conduction band positions of $LiAlTe_2$, $LiGaTe_2$, and $LiInTe_2$ decrease sequentially. In particular, $LiInTe_2$ forms a type-II band offset with $AgAlTe_2$, where the offsets are 0.229 and 0.197 eV for valence and conduction bands, respectively. This indicates that the light-generated electrons and holes can be separated efficiently at the interface between $AgAlTe_2$ and $LiInTe_2$. In addition, our calculated carrier effective masses for $LiInTe_2$ are $m^*_{001} = 0.25\ m_e$, $m^*_{100} = 0.21\ m_e$, and $m^*_{110} = 0.22\ m_e$ for electrons, which should be correlated with the isotropy of In-s state at CBM, and $m^*_{001} = 0.19\ m_e$, $m^*_{100} = 0.59\ m_e$, and $m^*_{110} = 0.59\ m_e$ for holes, which should be related to the anisotropy of Te p-states at the VBM (as shown in the PDOS in Fig. S2). The small effective carrier masses are beneficial for an effective optical response and carrier separation. Based on the criteria of ideal main bandgap for the IBSC, light carrier effective masses, lattice constant, and band offset matching with $AgAlTe_2$, $LiInTe_2$ is selected as the

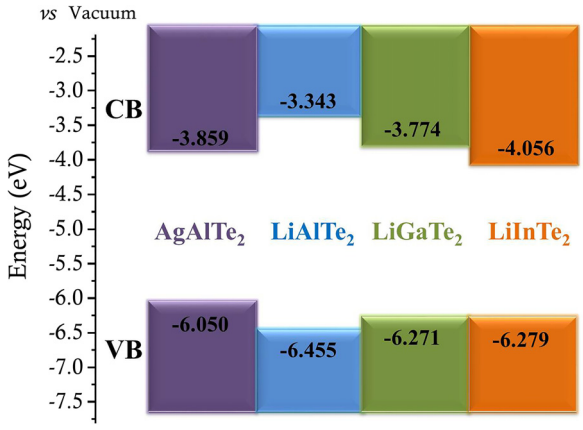

FIG. 1. The band edge positions relative to vacuum of $AgAlTe_2$, $LiAlTe_2$, $LiGaTe_2$, and $LiInTe_2$. Here, the bandgaps from our HSE06 calculations are adopted. There is a type-II band offset between $AgAlTe_2$ and $LiInTe_2$.

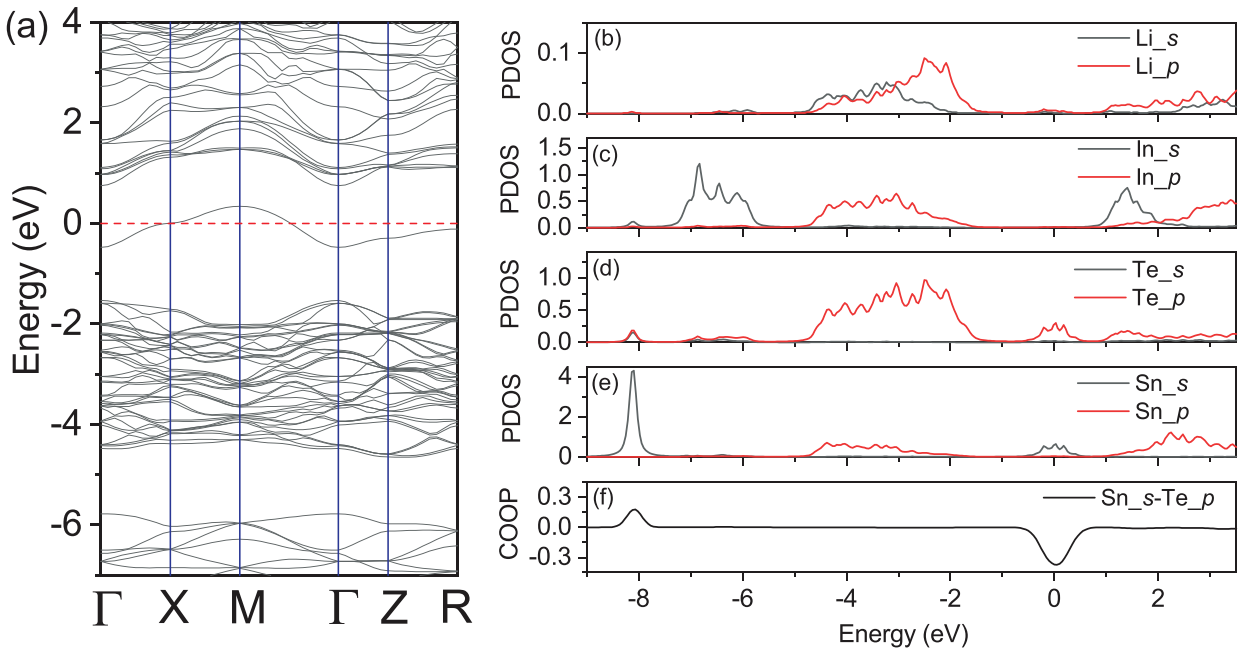

FIG. 2. The calculated band structure of Sn-doped $LiInTe_2$ (a) and the corresponding partial density of states (PDOS) of Li (b), In (c), Te (d), and Sn (e) and the COOP (f) between Sn-*s* and Te-*p* states. The Fermi energy level is set to zero.

component of the heterojunction to match $AgAlTe_2$ for the design on the tandem intermediate band absorber in this work.

As in the $AgAlTe_2$ case, doping of group-IV (Si, Ge, and Sn) elements at the In site is considered as the defects to produce a partially filled intermediate band in the main bandgap of $LiInTe_2$ since each of these atoms has one residual delocalized *s* electron and may form a band when heavily doped. Fortunately, the half-filled and isolated IBs are introduced in the bandgap of $LiInTe_2$ when any of these group-IV (Si, Ge, and Sn) elements are doped, as shown in Figs. 2(a) and S3. Unlike the flat intermediate band originated from *d*-orbitals,[33,34] the intermediate bands in Si, Ge, and Sn-doped $LiInTe_2$ are broad and show delocalized characteristic. As listed in Table I, the widths of the IBs are 0.733–0.888 eV, which are close to the optimal width (0.825 eV) of the intermediate band[35] according to the balance between the positive effect of recombination suppression and the negative effect of optical absorption reduction. Figures 2(b)–2(f) show the PDOS of Li, In, Te, Sn, and the crystal orbital overlap populations (COOP)[36] between Sn-*s* and Te-*p* states in Sn-doped $LiInTe_2$. The components of the original VB and CB do not change remarkably after Sn-doping in $AgAlTe_2$. The IB in the main bandgap mainly comes from Sn-*s* and Te-*p* states. Based on the analysis of COOP, we have learned that the IB results from the antibonding states between Sn-*s* states and Te-*p* states, while the corresponding bonding states are located around −8 eV below the Fermi level, as shown in Fig. 2(f). This is in line with the origin of the IB in Sn-doped $AgAlTe_2$. The wave function square of the IB in Sn-doped $LiInTe_2$ also shows antibonding and delocalized characters (c.f. Fig. S4), in line with the analyses of PDOS and COOP. Therefore, the IBs in different doped systems have a similar shape and are all delocalized, although the detailed position of IBs shifts from each other in the main bandgap for the various group-IV dopants (as shown in Fig. 5). The IB induced by Si-doping is higher in energy than those from Ge- and Sn-doping. The IB relative energy positions can be explained by our earlier illustrations based on bonding/antibonding attribution and atomic orbital energy as for group-IV (Si, Ge, and Sn)-doped $AgAlTe_2$.[21]

The sub-bandgaps in various doped systems possess different widths (c.f. Table I) due to different IB positions, thus affecting the theoretical efficiency of the IBSC directly. The main bandgap of pure

TABLE I. Widths of the original main bandgap, sub-bandgaps, and IB (unit: eV), as well as the theoretical efficiency at one sun concentration in pure and (Si, Ge, and Sn)-doped $LiInTe_2$.

Systems	Original main bandgap	Sub-band gap1 (VBM-E_f)	Sub-band gap2 (E_f-CBM)	Width of the IB	Theoretical efficiency
$LiInTe_2$	2.223	N/A	N/A	N/A	21%
Si-doped	2.329	1.926	0.403	0.733	30%
Ge-doped	2.304	1.396	0.908	0.737	45%
Sn-doped	2.286	1.540	0.746	0.888	43%

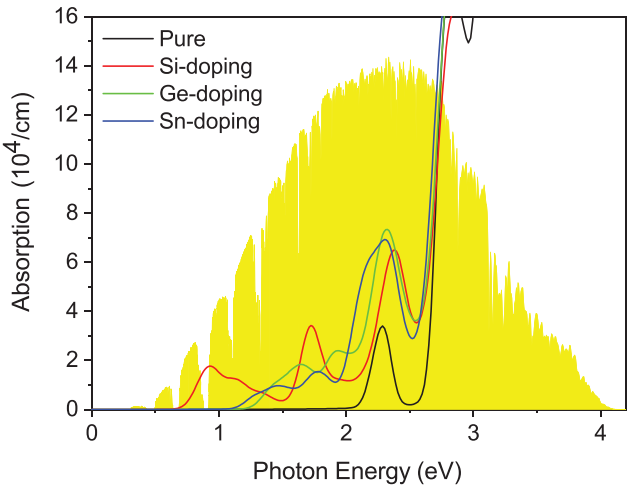

FIG. 3. Absorption coefficients of pure $LiInTe_2$ and (Si, Ge, and Sn)-doped $LiInTe_2$. The reference air-mass 1.5-solar spectral irradiance[38] is plotted in yellow.

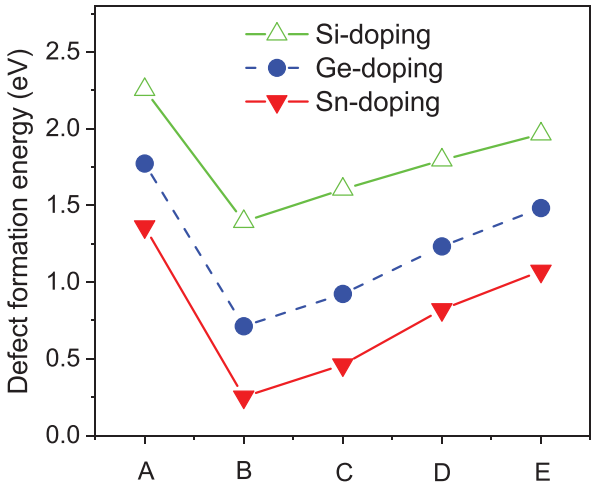

FIG. 4. Formation energies of Si, Ge, and Sn substituting at the In site in $LiInTe_2$ as a function of the chemical potential at points A, B, C, D, and E, which represent five extreme conditions in the allowed chemical potential ranges (in FIG. S5) for a stable $LiInTe_2$ with consideration of competing compounds.

$LiInTe_2$ is a little too large as the absorber for the single-junction solar cell and its theoretical efficiency is just 21%.[37] Ge- and Sn-doped $LiInTe_2$ have a suitable IB position and then the corresponding widths of sub-bandgap and main bandgap (c.f. Table I) can have a suitable distribution in the range of the solar light spectrum. The theoretical efficiencies of Ge- and Sn-doped $LiInTe_2$ are estimated to be 45% and 43%,[37] respectively, close to the maximum (46%) of the theoretical efficiency[11] of the IBSC with one IB. Figure 3 shows the absorption coefficient of pure and (Si, Ge, and Sn)-doped $LiInTe_2$. Obviously, the absorption coefficients of the doped systems can fulfill the absorption of photons with different energies and are enhanced in the visible light region and then cover the solar radiation spectrum effectively. Therefore, Ge and Sn are suitable dopants for $LiInTe_2$ to produce an IB, according to the induced IB position and widths of sub-bandgaps.[37]

In order to produce an IB other than the localized impurity level in the doped systems, the samples generally need to be heavily doped. To give an estimation on the possibility of realizing a large doping concentration of group-IV dopants in $LiInTe_2$, the defect formation energies on Si, Ge, or Sn substituting at the In site are calculated. The details on the calculations of defect formation energy are described in the supplementary material. Figure 4 shows the formation energies of Si, Ge, and Sn doping at the In site in $LiInTe_2$ under different chemical potential conditions. Sn-doping always has the lowest formation energy than Si and Ge doping when taking elemental Si, Ge, and Sn bulks as the dopant sources. It is hard to take Si (Ge) atoms from crystal Si (Ge) into $LiInTe_2$ owing to the strong covalent bonding in Si (Ge) bulk, while it is easier to take Sn atoms from crystal Sn into $LiInTe_2$ due to the relatively weak metallic bond in the Sn bulk. The defect formation energies reach the minimum under Te-rich and In-poor conditions, which would be the suitable growth condition. The lowest formation energies for Si_{In}, Ge_{In}, and Sn_{In} are 1.39, 0.71, and 0.25 eV, respectively. By employing the Boltzmann distribution law and setting the prepared temperature T of 1000 K,[39] the Sn_{In} and Ge_{In} doping concentration can reach ~5.6% and 0.03% under equilibrium conditions, respectively. The doping concentration can be even higher, away from the solid solubility limit,[40] as semiconductor samples can be prepared by non-equilibrium processes[41] such as implantation and molecular beam epitaxy. Therefore, we expect that the IB can be realized by Sn doping at the In site in $LiInTe_2$.

The band edge positions are expected to change compared to the pure system when various elements are doped heavily in $LiInTe_2$. The band offsets among the undoped and doped $LiInTe_2$ are calculated by the traditional approach,[42] i.e., aligned by the average potentials of host elements far away from the dopant. Combined with the band offset between pure $AgAlTe_2$ and $LiInTe_2$ (in Fig. 1), we can get the band offsets of various hosts with different dopants in Fig. 5. Following our

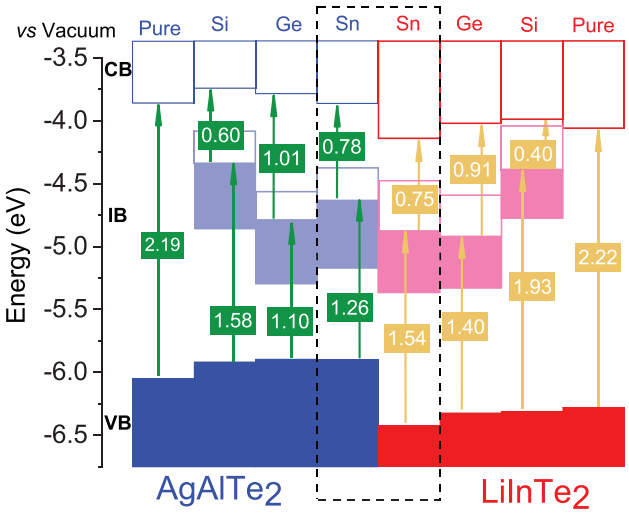

FIG. 5. The band energy positions relative to vacuum in pure and group-IV (Si, Ge, and Sn)-doped $AgAlTe_2$ and $LiInTe_2$. Here, the width of the main bandgap of pure compounds and the widths of sub-bandgaps of the doped systems (unit: eV) are labeled. The main bandgap of the doped systems can be obtained by adding the two sub-bandgaps. The interface of Sn-doped $AgAlTe_2$ and $LiInTe_2$ is highlighted in the dashed black line.

earlier work,[21] Sn-doped $AgAlTe_2$ is set as primary part of the tandem intermediate band absorber according to the suitable sub-bandgaps and the low defect formation energy. Our former work[21] also indicated that the band edge positions of $AgAlTe_2$ would not show a remarkable change after IV-group atom doping. Then, the type-II band offset between $AgAlTe_2$ and $LiInTe_2$ can be maintained after IV-group atom doping. One can observe that the VB, IB, and CB from both Sn-doped $LiInTe_2$ and Ge-doped $LiInTe_2$ have lower energy positions than those from Sn-doped $AgAlTe_2$. Since the positions of their Fermi energy levels do not show a significant variation, the partially filled IB can be preserved after the electron transfer when the heterojunction is formed. Therefore, from the band offset point of view, both Sn-doped $LiInTe_2$ and Ge-doped $LiInTe_2$ are suitable as another part of the heterojunction. Specifically, the conduction band offset and valence band offset between Sn-doped $AgAlTe_2$ and Sn-doped $LiInTe_2$ are 0.28 and 0.52 eV, respectively, which are slightly greater than those between rutile and anatase TiO_2 (i.e., 0.22 and 0.39 eV, respectively).[43] The band offsets are regarded to account for the efficient carrier separation and driving force for the increased photoactivity in rutile-anatase composite materials.[43] Therefore, we expect that it can have an efficient electron-hole separation at the interface of Sn-doped $AgAlTe_2$ and $LiInTe_2$. In addition, thin films $AgAlTe_2$[44] and $LiInTe_2$[45] have been grown by different experimental groups and large Sn doping concentrations in chalcopyrite compounds like 25% in Sn-doped $CuInSe_2$,[46] 8% in Sn-doped $CuAlS_2$,[47] and 6% in Sn-doped $CuGaSe_2$[48] have been reported experimentally. Considering the reported experimental results, low defect formation energies of Sn_{In} in $LiInTe_2$ and Sn_{Al} in $AgAlTe_2$(0.24 eV)[21] and less dopant types in the heterojunction, Sn-doped $AgAlTe_2$, and $LiInTe_2$ are expected to be convenient for the heterojunction growth. Although it contains some rare elements like Te (0.001 ppm in Earth's crust) and Ag (0.075 ppm in Earth's crust)[49] and some expensive elements like Li ($85.6/kg), In ($167/kg), and Ag ($521/kg),[49] the thin film heterojunction would not need a large amount of raw materials in a single solar cell module and the cost is normally decreased substantially once a technology has been established (e.g., LED lamps[50] and Li batteries[51]). Therefore, Sn-doped $AgAlTe_2$ and $LiInTe_2$ heterojunctions, which will have two main bandgaps and four sub-bandgaps, are suggested as the tandem intermediate band absorber.

In summary, we have studied the electronic structures of $LiXTe_2$ (X = Al, Ga, and In) and group-IV (Si, Ge, and Sn)-doped $LiInTe_2$ by first-principles calculations based on the hybrid HSE06 functional. It is found that $LiInTe_2$ is suitable to form a heterojunction with $AgAlTe_2$, as they have excellent lattice match and form a type-II band offset. It is also revealed that Sn is easily doped at the In site with a concentration up to ~5.6% and produce an IB. The absorption coefficient of Sn-doped $LiInTe_2$ can cover the solar light spectrum effectively, with the estimated theoretical efficiency of 43%.[37] Moreover, the type-II band offset is maintained between $AgAlTe_2$ and $LiInTe_2$ when both are heavily doped with Sn. Consequently, an absorber combining *tandem* and *IB* approaches was proposed to overcome the Shockley–Queisser limit, as exemplified with Sn-doped $AgAlTe_2$ and $LiInTe_2$. Moreover, our proposed model will stimulate the research interest to explore the tandem intermediate band absorber from low-cost and nontoxic compounds.

See the supplementary material for the calculated and referenced lattice parameters and bandgaps, the calculated band structures for $LiAlTe_2$, $LiGaTe_2$, and $LiInTe_2$, the partial density states of $LiInTe_2$, the band structures of Si- and Ge-doped $LiInTe_2$, the wave function square of the IB in Sn-doped $LiInTe_2$, and the calculation details of this work.

This work was financially supported by the National Natural Science Foundation of China (Grant Nos. 61664003, 61964002, and 12074126), the Hundred-Talent Program in Guangxi Province, Innovation-Driven Development Foundation of Guangxi Province (Grant No. AA17204063), and the Swedish Foundation for Strategic Research (No. RMA15-0030). We acknowledge the National High-Performance Computing Center Nanning Branch and Multifunctional Computer Center of Guangxi University and Swedish National Infrastructure for Computing for providing access to supercomputer resources.

DATA AVAILABILITY

The data that support the findings of this study are available from the corresponding author upon reasonable request.

REFERENCES

[1]N. S. Lewis, Science **315**, 798 (2007).
[2]K. L. Chopra, P. D. Paulson, and V. Dutta, Prog. Photovoltaics Res. Appl. **12**, 69 (2004).
[3]P. Jackson, R. Wuerz, D. Hariskos, E. Lotter, W. Witte, and M. Powalla, Phys. Status SolidiRRL **10**, 583 (2016).
[4]E. H. Jung, N. J. Jeon, E. Y. Park, C. S. Moon, T. J. Shin, T. Y. Yang, J. H. Noh, and J. Seo, Nature **567**, 511 (2019).
[5]W. Shockley and H. J. Queisser, J. Appl. Phys. **32**, 510 (1961).
[6]A. D.Vos, J. Phys. D: Appl. Phys. **13**, 839 (1980).
[7]A. Luque and A. Martí, Phys. Rev. Lett. **78**, 5014 (1997).
[8]A. Luque, A. Martí, and C. Stanley, Nat. Photonics **6**, 146 (2012).
[9]S. Kahmann and M. A. Loi, J. Mater. Chem. C **7**, 2471 (2019).
[10]J. F. Geisz, R. M. France, K. L. Schulte, M. A. Steiner, A. G. Norman, H. L. Guthrey, M. R. Young, T. Song, and T. Moriarty, Nat. Energy **5**, 326 (2020).
[11]A. S. Brown and M. A. Green, J. Appl. Phys. **92**, 1329 (2002).
[12]X. Lv, S. Yang, M. Li, H. Li, J. Yi, M. Wang, G. Niu, and J. Zhong, Sol. Energy **103**, 480 (2014).
[13]P. Chen, M. Qin, H. Chen, C. Yang, Y. Wang, and F. Huang, Phys. Status Solidi. A **210**, 1098 (2013).
[14]B. Marsen, S. Klemz, T. Unold, and H. W. Schock, Prog. Photovoltaics Res. Appl. **20**, 625 (2012).
[15]C. Yang, M. Qin, Y. Wang, D. Wan, F. Huang, and J. Lin, Sci. Rep. **3**, 1286 (2013).
[16]K. Hu, D. Wang, W. Zhao, Y. Gu, K. Bu, J. Pan, P. Qin, X. Zhang, and F. Huang, Inorg. Chem. **57**, 3956 (2018).
[17]P. Wahnón, J. C. Conesa, P. Palacios, R. Lucena, I. Aguilera, Y. Seminovski, and F. Fresno, Phys. Chem. Chem. Phys. **13**, 20401 (2011).
[18]C. Tapia, S. P. Berglund, D. Friedrich, T. Dittrich, P. Bogdanoff, Y. Liu, S. Levcenko, T. Unold, J. C. Conesa, A. L. D. Lacey, M. Pita, and S. Fiechter, J. Phys. Chem. C **120**, 28753 (2016).
[19]T. Tanaka, M. Miyabara, Y. Nagao, K. Saito, Q. Guo, M. Nishio, K. M. Yu, and W. Walukiewicz, IEEE J. Photovoltaics **4**, 196 (2014).
[20]E. Antolín, C. Chen, I. Ramiro, J. Foley, E. López, I. Artacho, J. Hwang, A. Teran, E. Hernández, C. Tablero, A. Martí, J. D. Phillips, and A. Luque, IEEE J. Photovoltaics **4**, 1091 (2014).
[21]D. Huang, J. W. Jiang, J. Guo, Y. J. Zhao, R. Chen, and C. Persson, Semicond. Sci. Technol. **32**, 065007 (2017).
[22]L. Isaenko, P. Krinitsin, V. Vedenyapin, A. Yelisseyev, A. Merkulov, J.-J. Zondy, and V. Petrov, Cryst. Growth Des. **5**, 1325 (2005).
[23]A. Uruno, Y. Takeda, T. Inoue, Y. Takeda, and M. Kobayashi, Phys. Status Solidi. C **13**, 413 (2016).
[24]L. Isaenko, I. Vasilyeva, A. Merkulov, A. Yelisseyev, and S. Lobanov, J. Cryst. Growth **275**, 217 (2005).

[25]A. H. Reshak and M. G. Brik, J. Alloys Compd. **675**, 355 (2016).
[26]H. Xiao, J. Tahir-Kheli, and W. A. Goddard III, J. Phys. Chem. Lett. **2**, 212 (2011).
[27]A. H. Reshak and W. Khan, J. Alloys Compd. **592**, 92 (2014).
[28]V. A. Ha, G. Yu, F. Ricci, D. Dahliah, M. J. Setten, M. Giantomassi, G. M. Rignanese, and G. Hautier, Phys. Rev. Mater. **3**, 034601 (2019).
[29]A. Cohen, P. Mori-Sánchez, and W. Yang, Science **321**, 792 (2008).
[30]M. Ley, J. Boudaden, and Z. T. Kuznicki, J. Appl. Phys. **98**, 044905 (2005).
[31]W. Wang, A. S. Lin, and J. D. Phillips, Appl. Phys. Lett. **95**, 011103 (2009).
[32]D. Huang, Z. Ju, H. Ning, C. Li, C. Yao, and J. Guo, Mater. Chem. Phys. **148**, 882 (2014).
[33]J. Hashemi, A. Akbari, S. Huotari, and M. Hakala, Phys. Rev. B **90**, 075154 (2014).
[34]M. Han, X. Zhang, and Z. Zeng, RSC Adv. **4**, 62380 (2014).
[35]M. Y. Levy and C. Honsberg, Phys. Rev. B **78**, 165122 (2008).
[36]S. Maintz, V. L. Deringer, A. L. Tchougréeff, and R. Dronskowski, J. Comput. Chem. **37**, 1030 (2016).
[37]S. E.Jenks, "Quantum Dot Intermediate Band Solar Cells: Design Criteria and Optimal Materials" Doctoral thesis (Drexel University, 2012).
[38]See https://www.nrel.gov/grid/solar-resource/spectra-am1.5.html for "Solar Spectral Irradiance: Air Mass 1.5 spectra."
[39]G. Kühn, B. Schumann, D. Oppermann, H. Neumann, and H. Sobotta, Z. Anorg. Allg. Chem. **531**, 61 (1985).
[40]M.Wang, A. Debernardi, Y. Berencén, R. Heller, C. Xu, Y. Yuan, Y. Xie, R. Böttger, L. Rebohle, and W. Skorupa, Phys. Rev. Appl. **11**, 054039 (2019).
[41]C. G. Van de Walle and J. Neugebauer, J. Appl. Phys. **95**, 3851 (2004).
[42]W. J. Yin, H. Tang, S. H. Wei, M. M. Al-Jassim, J. Turner, and Y. Yan, Phys. Rev. B **82**, 045106 (2010).
[43]D. O. Scanlon, C. W. Dunnill, J. Buckeridge, S. A. Shevlin, A. J. Logsdail, S. M.Woodley, C. R. A. Catlow, M. J. Powell, R. G. Palgrave, I. P. Parkin, G. W. Watson, T. W. Keal, P. Sherwood, A. Walsh, and A. A. Sokol, Nat. Mater. **12**, 798 (2013).
[44]A. Uruno, A. Usui, and M. Kobayashi, J. Appl. Phys. **116**, 183504 (2014).
[45]B. Schumann, G. Nolze, and G. Kühn, Thin Solid Films **151**, 35 (1987).
[46]Y. C. Lin and H. J. Chen, Chin. J. Phys. **56**, 2022 (2018).
[47]C. Guo, C. Yang, Y. Xie, P. Chen, M. Qin, R. Huang, and F. Huang, RSC Adv. **6**, 40806 (2016).
[48]W. Fan, H. Yao, Y. Wang, and Q. Li, AIP Adv. **10**, 065031 (2020).
[49]See https://en.wikipedia.org/wiki/Prices_of_chemical_elements for "Abundance of Elements in Earth Crust and Prices of Chemical Elements."
[50]F. K. Yam and Z. Hassan, Microelectron J. **36**, 129 (2005).
[51]A. Manthiram, ACS Cent. Sci. **3**, 1063 (2017).